JOURNAL OF GEOPHYSICAL RESEARCH, VOL. 98, NO. D2, PAGES 2757–2765, FEBRUARY 20, 1993

On the Accuracy of the Eddington Approximation for Radiative Transfer in the Microwave Frequencies

CHRISTIAN KUMMEROW

Laboratory for Atmospheres, Goddard Space Flight Center, Greenbelt, Maryland

Radiative transfer calculations in the presence of clouds and precipitation simplify as the wavelengths of the radiation approach the Rayleigh scattering regime. In particular, the transfer of microwave radiation is often simpler than the equivalent calculations at shorter wavelengths because the order of quadrature and moments of the phase function needed for the treatment of scattering decrease as the wavelength increases. The purpose of this paper is to examine how well an Eddington approximation can reproduce brightness temperatures obtained from a more complete, N-stream discrete ordinate solution in the microwave regime. Radiation propagating through a plane parallel medium will be considered in this discussion. Although model discrepancies are complicated functions of the cloud constituents, the differences between an eight-stream discrete ordinate solution and an analytical Eddington solution were generally small, ranging from 0 to 6°K when only one uniform layer of hydrometeors was considered. When realistic, multilayered cloud hydrometeor profiles were used, the differences between these two models never exceeded 3°K over the entire range of microwave frequencies considered (6.6–183 GHz). The models agreed to within 0.2°K in the absence of scattering constituents.

1. INTRODUCTION

The detection and measurement of clouds and precipitation on a global scale is of great importance in a wide range of meteorological problems. One of the basic problems in this area is the effect of precipitation in the tropics and subtropics upon the Earth's large scale circulation patterns. Unfortunately, there is still today an almost complete lack of quantitative information regarding precipitation amounts and distributions over these regions. Indirect estimates of the global precipitation totals often disagree by 100% or more.

Infrared techniques developed in the past to infer precipitation from outgoing long wave radiation [e.g., *Arkin and Meisner*, 1987; *Inoue*, 1987; *Adler and Negri*, 1988] generally suffer from an imcomplete correlation between cold brightness temperatures and precipitation. Microwave rainfall retrievals, although fraught with their own problems, offer a much more direct relationship between brightness temperatures and precipitation. This is due to the fact that for all but the strongest convection, frequencies less than 35 GHz have the bulk of their signal originating from well within the rain layer itself. Understanding and simulating microwave brightness temperatures can thus lead to more physical rainfall retrieval schemes such as those developed by *Wilheit et al.* [1977], *Spencer* [1986], or *Hollinger et al.* [1987]. This paper will focus on the radiative transfer calculations needed to obtain the necessary relationships between brightness temperatures and rainfall rates. Its results, however, are general and may be applied to other problems of radiative transfer as well.

As the need to physically interpret microwave brightness temperatures increasese with more sophisticated retrieval algorithms, so does the need for fast, yet accurate radiative transfer calculations. To meet this demand, a number of plane parallel radiative transfer models dealing explicitly with microwave frequencies have been described in the literature. Some of the more widely referenced codes include the Eddington approximation described by *Wu and Weinman* [1984], an iterative scheme first described by *Wilheit et al.* [1977], as well as a multistream double-adding scheme with a complete treatment of polarization developed by *Evans and Stephens* [1990]. More general radiative transfer codes applicable to a wider range of frequencies are described by *Shettle and Weinman* [1970], *Coakley and Chylek* [1974], *Stephens* [1988], and *Stamnes et al.* [1988]. For microwave radiative transfer calculations through clouds and precipitation, however, the amount of detail needed in the transfer calculations in order to properly simulate brightness temperatures has never been fully documented.

With the recent launch of the Special Sensor Microwave/Imager (SSM/I) aboard the Defense Meteorological Satellite Program spacecraft [*Hollinger et al.*, 1987], the proposed Tropical Rainfall Measuring Mission [*Simpson et al.*, 1988], and the upcoming Earth Observing Systems mission, there has been considerable emphasis on measuring precipitation. A fast, yet accurate radiative transfer model is essential for this purpose. It is also important in a number of recent studies [e.g., *Mugnai and Smith*, 1988] which seek to gain insight into microwave brightness temperature/rain rate relations by simulating radiances through precipitation fields generated by cloud dynamical models. Such studies require a very large number of radiative transfer calculations to track the spatial as well as temporal development of brightness temperatures. While most radiative transfer solutions account for emission and absorption processes in much the same way, this is not the case for multiple scattering which is important in the case of microwave radiation propagating through precipitation. The major differences between the solutions in this case becomes the ability of the radiative transfer solution to properly capture the angular distribution of the radiation. In this paper, the accuracy of two Eddington solutions which consider only the second moment of the angular distribution will be examined by comparing them to each other, and to a discrete ordinate solution which con-

Paper number 92JD02472.

siders any number of moments but is also computationally much slower. While there are a number of other potential solutions which could have been compared (e.g., the adding-doubling codes of *Wilheit et al.* [1977] or *Evans and Stephens* [1990], or multiple order of scattering methods), it was felt that this would add little to the focus of this paper. These codes generally show almost perfect agreement among themselves for the type of problem considered here, but all require increased computational resources.

All solutions are for time-independent transfer calculations in vertically inhomogeneous, nonisothermal, plane parallel media. The physical processes included are thermal emission, absorption, scattering and emission at the lower boundary.

2. MODELS

Basic Equations

The purpose of this section is to provide a basic framework for the radiative transfer models. No effort is made to develop the theories fully as they are well described in the literature. Instead, this section is intended to serve as an introduction to microwave radiative transfer, and to set forth notation. With this in mind, the equation describing the transfer of monochromatic radiation at frequency v through a plane parallel medium is given by

$$\cos\theta \frac{dI_v(z,\theta,\phi)}{dz} = -k_v(z)[I_v(z,\theta,\phi) - J_v(z,\theta,\phi)] \tag{1}$$

where $I_v(z, \theta, \phi)$ is the radiance at height z, propagating in the direction of θ, ϕ; k_v is the extinction coefficient of the medium, and $J_v(z, \theta, \phi)$ is the source function which is given by

$$J_v(z,\theta,\phi) = [1 - a_v(z)]B_v[T(z)] + \frac{a_v(z)}{4\pi}\int_0^{2\pi}\int_{-1}^{+1} P_v(\theta,\phi;\theta',\phi') \cdot I_v(z,\theta',\phi')\, d(\cos\theta')\, d\phi' \tag{2}$$

where $a_v(z)$ is the albedo for single scattering, $T(z)$ is the abiment temperature of the medium, $B_v[T(z)]$ is the Planck function at frequency v and temperature $T(z)$, and $P(\theta; \phi; \theta', \phi')$ is the phase function for scattering of radiation from direction θ, ϕ into θ', ϕ'. In the microwave regime at typical tropospheric temperatures, the Planck function is virtually a linear function of temperature. It is therefore common to replace $B_v[T(z)]$ by $T(z)$, which implies that the radiances must be interpreted as brightness temperatures T_B, rather than a power per unit area.

Eddington Approximation

In the plane parallel Eddington approximation, radiances are expanded in a series of Legendre and associated Legendre functions:

$$I(z,\theta,\phi) = I_0(z) + I_1(z)\cos\theta + \cdots \tag{3}$$

If the series is terminated as shown, and the phase function is similarly expanded in Legendre polynomials:

$$P(\cos\vartheta) = \sum_{l=0}^{N} \omega_l P_l(\cos\vartheta) = 1 + \omega_1\cos\vartheta + \cdots \tag{4}$$

where ϑ is the angle from θ', ϕ' to θ, ϕ, then the source function $J(z, \theta, \phi)$ can be written as

$$J(z,\theta,\phi) = [1 - a(z)]T(z) + a(z)[I_0(z) + g(z)I_1(z)\cos\theta] \tag{5}$$

where the asymmetry factor g is given by $g = \omega_1/3$. Using this expression for the source function, (1) can be shown [see *Weinman and Davies*, 1978] to reduce to the following expression for the isotropic component of the diffuse radiance I_0:

$$\frac{d^2I_0(z)}{dz^2} = \lambda^2(z)[I_0(z) - T(z)] \tag{6}$$

where $\lambda^2(z) = 3k^2(z)[1 - a(z)][1 - a(z)g(z)]$.

In practice, the simplest solution occurs when k, a, and g are independent of height, and $T(z)$ is written as $T_0 + \Gamma z$, where Γ is the lapse rate of the atmosphere. Equation (6) then becomes a simple second-order differential equation. It has a solution of the form $I_0(z) = D_+ \exp(\lambda z) + D_- \exp(-\lambda z) + T_0 + \Gamma z$, where D_+ and D_- are constants to be determined from the boundary conditions. In order to exploit this simplification, clouds are generally divided into n homogeneous layers such that the above conditions are approximately satisfied in each layer. The downward flux at the top of the cloud determines the upper boundary condition, while the upward flux at the bottom of the cloud determines the lower boundary condition. Flux continuity at the layer interfaces provides the remaining boundary conditions if more than one layer is assumed. This solution will be referred to as the analytical Eddington solution.

A second approach, which is due to *Wu and Weinman* [1984], makes use of (1)–(5) to obtain a pair of first-order equations for I_0 and I_1:

$$\frac{dI_0(z)}{dz} = -k(z)[1 - a(z)g(z)]I_1(z) \tag{7a}$$

$$\frac{dI_1(z)}{dz} = -3k(z)[1 - a(z)][I_0(z) - T(z)] \tag{7b}$$

In this solution, the atmosphere is stratified into $2n + 1$ levels. The I_0 are defined at the layer boundaries while the I_1 are defined at the center of each layer. Equations (7*a*) and (7*b*) are rewritten in finite difference form and the solution is sought numerically. This solution will be referred to as the finite difference Eddington solution. Details can be found in *Wu and Weinman* [1984].

To obtain the radiation emerging at the top of the atmosphere, we define z_0 as the surface and z_n as the top of the atmosphere, with average layer quantities ranging from 1 to n. Azimuthal dependence may enter into the radiative transfer problem from three different sources: External, anisotropic sources of radiation, horizontally finite clouds or azimuthal dependence of the surface reflectivity. Because none of these cases are considered here, the ϕ dependence in (1) may be omitted. For a Lambertian surface, and no ϕ

dependence in the solution, the radiances that would be measured at the top of the first layer in both solutions is given by

$$I(z_1, \theta) = \varepsilon T_s \exp\left[\frac{-k_1(z_1 - z_0)}{\cos\theta}\right] + \frac{2}{\pi}\int_0^{\pi/2}(1-\varepsilon) \cdot I(z_0, -\theta') \exp\left[\frac{-k_1(z_1 - z_0)}{\cos\theta}\right]\cos\theta'\, d\theta' + \int_0^{z_1} J_1(z, \theta)k_1 \exp\left[\frac{-k_1(z_1 - z)}{\cos\theta}\right] dz/\cos\theta \quad (8a)$$

were ε is emissivity, T_s the temperature of the surface, and $I(z_0, -\theta)$ is defined in (9). The first term in (8a) is the surface contribution to the upwelling radiance. The second term represents the contribution of the downwelling radiance which is reflected at the surface, while the last term corresponds to the component of the radiation within the atmosphere propagating upward. The radiation emerging from layers above the first layer may be calculated easily by the recursion relation

$$I(z_n, \theta) = I(z_{n-1}, \theta) \exp\left[\frac{-k_n(z_n - z_{n-1})}{\cos\theta}\right] + \int_{z_{n-1}}^{z_n} J_n(z, \theta)k_n \exp\left[\frac{-k_n(z_n - z)}{\cos\theta}\right] dz/\cos\theta \quad (8b)$$

The downwelling radiance $I(z_0, -\theta)$ defined in (8a) can similarly be found from a recursion relation. At the top of the atmosphere, $I(z_0, -\theta)$ is simply given by the cosmic background radiation, namely, $I(z_0, -\theta) = 2.7$°K. Lower layers may then be computed through

$$I(z_{n-1}, -\theta) = I(z_n, -\theta) \exp\left[\frac{-k_{n-1}(z_{n-1} - z_n)}{\cos(-\theta)}\right] + \int_{z_n}^{z_{n-1}} J_{n-1}(z, -\theta)k_{n-1} \cdot \exp\left[\frac{-k_{n-1}(z_{n-1} - z)}{\cos(-\theta)}\right] dz/\cos(-\theta) \quad (9)$$

Discrete Ordinate Model

The solution which will be described here is a summary of the formulation presented by *Stamnes et al.* [1988]. Their solution was chosen because a complete, well-documented radiative transfer code is available from the authors and was therefore ideally suited to make comparisons between the models. In order to keep this article self-consistent, however, their notation has been changed wherever necessary to match the notation used in the previous section.

In the discrete ordinate solution, the integral in (2) is replaced by a Gaussian quadrature. In this formulation, (1) may be written as

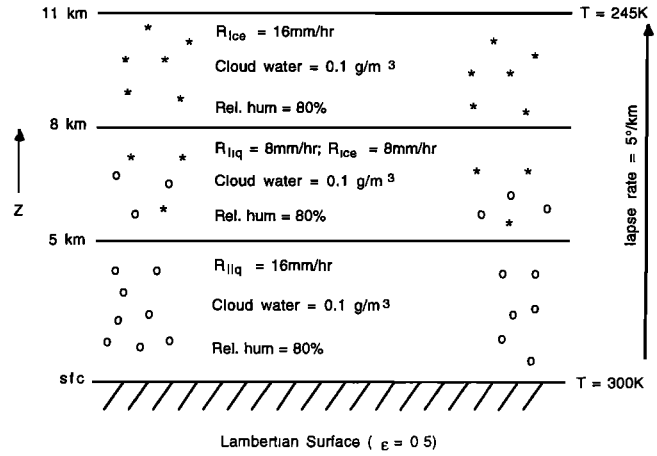

Fig. 1. Schematic view of the cloud used to test radiative transfer solutions.

$$\frac{\mu_i}{k}\frac{dI(z, \mu_i)}{dz} = -I(z, \mu_i) + (1-a)B_v[T(z)] + \sum_{j=-N;j\neq 0}^{j=N} w_j D(\mu_i, \mu_j)I(z, \mu_j) \quad (10)$$

where μ_i and w_i are quadrature points and weights, respectively, $2N$ is the number of discrete streams, and $D(\mu_i, \mu_j)$ are defined in terms of the first N moments of the phase function defined in (4), and given by

$$D(\mu_i, \mu_j) = \frac{a}{2}\sum_{l=0}^{2N-1}(2l+1)\omega_l P_l(\mu_i)P_l(\mu_j) \quad (11)$$

where

$$\omega_l = \frac{1}{2}\int_{-1}^{+1} P_l(\mu)P(\cos\vartheta)\, d\mu \quad (12)$$

To obtain a solution to (10), the atmosphere is again layered such that the scattering coefficients are constant within each layer. The solution can then be found by applying the proper boundary conditions at the top and bottom of the cloud, as well as the layer interfaces. Numerical solutions are sought to (10). The discrete solutions may then be used to derive explicit expressions for the source function (2), which can be integrated analytically to obtain the radiance $I(z, \theta)$ anywhere within a layer. In a multilayer medium, the calculation of the radiance at the top of the cloud propagating in the direction of the satellite then follows the same procedure described for the Eddington approximation.

3. MODEL COMPARISONS

Basic Model

A simple, three-layer cloud model shown in Figure 1 is used to make comparisons between the radiative transfer solutions. The simplicity of the cloud structures insures not only that physical insight is retained, but it also makes it possible to give explicit values for all the input parameters into the radiative transfer solutions. This is important so that

TABLE 1. Scattering Parameters Associated With the Three-Layer Cloud Model Shown in Figure 1

	Frequency, GHz					
	6.6	10.7	18.0	37.0	85.6	183.0
			0- to 5-km Layer			
k_{liquid}	0.022	0.098	0.321	1.17	2.73	15.4
a_{liquid}	0.040	0.069	0.168	0.391	0.461	0.096
g_{liquid}	0.091	−0.017	−0.082	0.010	0.276	0.539
			5- to 8-km Layer			
k_{mixed}	0.012	0.038	0.125	0.596	2.04	9.46
a_{mixed}	0.024	0.056	0.145	0.361	0.557	0.255
g_{mixed}	0.045	0.014	−0.010	0.091	0.394	0.522
			8- to 11-km Layer			
k_{ice}	0.002	0.006	0.023	0.183	1.45	5.90
a_{ice}	0.064	0.167	0.383	0.751	0.916	0.464
g_{ice}	0.012	0.031	0.087	0.305	0.516	0.539

Values are in km^{-1}

other solutions may be compared with the results presented here.

The relative humidity in this simple model is set at 80% throughout the cloud. The nonprecipitating cloud liquid water is also assumed constant, with a value of 0.1 g m^{-3} throughout the cloud. The Earth's surface is assumed to be Lambertian with an emissivity of 0.5. Unless otherwise noted, a viewing angle of 50° is used in the subsequent calculations. This particular angle was chosen because it closely resembles the viewing angle of existing sensors. The water vapor absorption is calculated according to *Ulaby et al.* [1981]. The oxygen absorption is calculated according to *Staelin* [1966], while the cloud liquid water extinction is found from Rayleigh theory. The hydrometeor profile is assumed to be a constant 16 mm h^{-1} within the cloud. From the surface to 5 km, the hydrometeors are assumed liquid. From 5 to 8 km, the hydrometeors are equally divided among liquid and frozen drops, while all the hydrometeors are assumed frozen between 8 and 11 km. The size distribution is assumed to follow that of *Marshall and Palmer* [1948]. Mie theory is used to obtain the extinction coefficient k, the albedo for single scattering a, and the phase function $P(\theta)$ from which the asymmetry factor g $(=\omega_{1/3})$, is calculated from (12).

If the extinctions due to the gaseous and nonprecipitating cloud components in the atmosphere are grouped into k_{atm} (i.e., $k_{atm} = k_{water\ vapor} + k_{oxygen} + k_{cloud\ water}$), then the scattering coefficients entering into the radiative transfer calculations are given by

$$k_{tot} = k_{liq} + k_{ice} + k_{atm}$$

$$a_{tot} = (a_{liq} \times k_{liq} + a_{ice} \times k_{ice})/k_{tot} \quad (13)$$

$$g_{tot} = (g_{liq} \times a_{liq} \times k_{liq} + g_{ice} \times a_{ice} \times k_{ice})/(a_{tot} \times k_{tot})$$

The numerical values of these quantities are given explicitly for all three layers in Table 1. This, along with the first eight moments of the phase function expansion given in Table 2, should allow the interested users of a radiative transfer solution to compare their answers to the ones presented here without having to exactly duplicate the input parameter calculations.

TABLE 2. Moments of the Phase Function Expansion Needed to Calculate the Brightness Temperatures Presented in Table 1

		Phase Function Moment								
Frequency	Layer	0	1	2	3	4	5	6	7	8
6.6	1	1.0000	0.0909	0.1004	0.0007	0.0000	0.0000	0.0000	0.0000	0.0000
	2	1.0000	0.0448	0.1001	0.0005	0.0000	0.0000	0.0000	0.0000	0.0000
	3	1.0000	0.0116	0.1000	0.0008	0.0000	0.0000	0.0000	0.0000	0.0000
10.7	1	1.0000	−.0170	0.0996	0.0018	0.0000	0.0000	0.0000	0.0000	0.0000
	2	1.0000	0.0145	0.1000	0.0013	0.0000	0.0000	0.0000	0.0000	0.0000
	3	1.0000	0.0305	0.1004	0.0021	0.0000	0.0000	0.0000	0.0000	0.0000
18.0	1	1.0000	−.0817	0.0967	0.0043	0.0001	0.0000	0.0000	0.0000	0.0000
	2	1.0000	−.0098	0.0994	0.0034	0.0001	0.0000	0.0000	0.0000	0.0000
	3	1.0000	0.0868	0.1034	0.0056	0.0002	0.0000	0.0000	0.0000	0.0000
37.0	1	1.0000	0.0096	0.0921	0.0124	0.0022	0.0003	0.0000	0.0000	0.0000
	2	1.0000	0.0905	0.1038	0.0111	0.0014	0.0001	0.0000	0.0000	0.0000
	3	1.0000	0.3054	0.1372	0.0219	0.0037	0.0004	0.0000	0.0000	0.0000
85.6	1	1.0000	0.2758	0.1522	0.0607	0.0286	0.0106	0.0042	0.0015	0.0005
	2	1.0000	0.3935	0.1874	0.0656	0.0248	0.0072	0.0027	0.0006	0.0002
	3	1.0000	0.5159	0.2520	0.1018	0.0423	0.0136	0.0064	0.0014	0.0009
183.	1	1.0000	0.5611	0.3767	0.2430	0.1576	0.0991	0.0624	0.0385	0.0237
	2	1.0000	0.5557	0.3413	0.1843	0.1088	0.0557	0.0348	0.0158	0.0111
	3	1.0000	0.5465	0.3543	0.1857	0.1207	0.0608	0.0449	0.0192	0.0173

TABLE 3. Brightness Temperatures Calculated Using an "Analytical" and a "Finite Difference" Eddington Approximation Without Regard to Instabilities Resulting From Large Optical Depths

	Frequency, GHz					
	6.6	10.7	18.0	37.0	85.6	183.0
T_B (analytical), °K	203.4	259.9	261.9	216.9	158.3	228.9
T_B (finite difference) three layers	201.6	255.1	251.4	180.0	65.7	72.2

Analytical and Finite Difference Eddington Comparison

It is of value to begin by comparing the analytical Eddington results to the difference results (Table 3). As noted in the previous section, the major differences between these two models is that the analytical approach solves a second-order equation exactly, while the finite difference approach solves two first-order equations for the diffuse radiance by numerical methods. The two solutions should therefore agree to within the errors introduced by the numerical method. There are, however, some conceptual differences with the particular finite difference solution proposed by *Wu and Weinman* [1984] which require special attention. Specifically, the Wu and Weinman solution requires that the scattering coefficients k, a, and g be specified not only for each layer, but also at the layer interfaces. While it is straightforward to use the average between two layers to represent the layer interface, it is not intuitively obvious what values should be used at the top and bottom of the cloud. In the brief illustration that follows, one half the value within the top and bottom layer was chosen to represent the values at the top and bottom of the cloud respectively. Unfortunately, the choice of boundary conditions may affect the calculated radiances.

Beyond the above-mentioned ambiguity, the finite difference approach of Wu and Weinman has a further shortcoming due to the numerical method itself. To illustrate this point, the solutions are inspected in the absence of thermal emission and scattering (i.e., Beer's law). In this case, the radiative transfer problem may be written as $dI(z)/dz = -k_{ext}I(z)$, which has the well-known solution $I(z) = I(0) \exp(-kz)$. In a layered atmosphere this solution may be expressed as $I_{i+1} = I_i \exp(-k\Delta z)$. If this same equation is written in finite difference form, however, the equation becomes $[I_{i+1}(z) - I_i(z)]/\Delta z = -kI_{i+1}(z)$. This equation has a solution of the form $I_{i+1} = I_i/(1 + k\Delta z)$. One can compare the analytical and finite difference solutions by expanding both solution. The expansion for the analytical solution is given by

$$I_{i+1} = I_i\left[1 + (-k\Delta z) + \frac{1}{2}(-k\Delta z)^2 + \frac{1}{6}(-k\Delta z)^3 + \cdots\right] \quad (14)$$

while the finite difference solution has the form

$$I_{i+1} = I_i[1 - k\Delta z + (k\Delta z)^2 - (k\Delta z)^3 + \cdots] \quad (15)$$

Thus, as can be seen from this simple analogy, the finite difference solution approaches the exact solution only if $(k\Delta z)$ is small enough that the second-order term in the expansion is negligible.

The effects of calculating brightness temperatures without first insuring that $(k\Delta z)$ is small can be illustrated quite well using the three-layer structure described in the previous section. As can be seen, the answers agree fairly well for the optically thinnest case (6.6 GHz), but extremely large differences exist at the higher frequencies, where $(k\Delta z)$ is considerably larger than unity. While the above problems may be corrected by subdividing layers until $(k\Delta z)$ is small, the repeated doubling of computational layers causes a four fold increase in computer requirements, both in memory as well as CPU time. In short, while the answer from both solutions should be equivalent, the finite difference method requires considerably more caution and generally greater computational resources than the analytical Eddington solution. Only the analytical solution is therefore considered in the subsequent comparisons.

Analytical and Discrete Ordinate Comparisons

The first comparison between the analytical Eddington solution and the discrete ordinate solution is for the three-layer model discussed in the previous section and shown in Figure 1. The input parameters k, a, and g are given in Table 1. For the discrete ordinate model, the phase function must be expanded in terms of its first n moments, where n is the total number of discrete streams considered in the calculations. Numerical values for those wishing to do further comparisons are given in Table 2.

Agreement between the two models appears excellent if four or more streams are used (Table 4). The four-stream solution does not do quite as well as the analytical Eddington solution in the 6.6 GHz case because the reflection from the Lambertian surface is limited to four streams in the discrete ordinary solution. For optically thicker clouds (10.7 GHz and higher), the effects from the surface diminish and the four-stream discrete ordinate solution appears to give the better results. The eight-stream solution seems to have converged to within 0.1°K of the true answer for all frequencies considered here.

Before proceeding with a careful comparison between these two models, it should be emphasized that the same scattering parameters are used for both models. The same input data specifying the cloud model characteristics are also used, thus guaranteeing that the differences in the calculated brightness temperatures are due solely to the radiative transfer solutions, and not due to differences in the input parameters.

In the following comparisons, there exists a tradeoff between the solutions. Although the discrete ordinate solution is more accurate, it requires significantly more computing time than the analytical Eddington solution. Thus, the reader interested in choosing a particular model must be able to see comparisons under a variety of circumstances. Unlike the finite difference approach which is clearly inferior to the analytical solution under all circumstances, careful consideration of the computing speed and desired accuracies must be weight to choose between the present models. Unless otherwise stated, the 8-stream solution is used to obtain answers for the discrete ordinate model.

Model comparisons were performed for a continuous range of optical thicknesses and viewing angles for three

TABLE 4. Comparisons Between an "Analytical" Eddington Approximation and an N-Stream Discrete Ordinate Solution

	Frequency, GHz					
	6.6	10.7	18.0	37.0	85.6	183.0
	Analytical Eddington Solution					
	203.4	259.9	261.9	216.9	158.3	228.9
	N-Stream Discrete Ordinate Solution					
Two stream*	206.0	264.4	262.1	214.0	151.8	226.8
Four stream	204.5	260.5	262.3	216.8	159.4	229.9
Eight stream	203.6	260.3	262.4	217.1	159.4	230.0
Sixteen stream	203.6	260.4	262.4	217.1	159.4	230.0

*The distributed code warns against using the two stream results. They are included here only to reiterate the warning.

selected values of the single scattering albedo a and three selected values for the asymmetry factor g. The surface was assumed Lambertian with an emissivity ε of 0.5 for all the following calculations. The single scattering albedo a was assigned values of 0.1, 0.5, and 0.9. The lower limit, $a = 0.1$, rather than the nonscattering solution, $a = 0$, was chosen because both radiative transfer solutions are identical in the nonscattering limit. Values of $a = 0.1$ thus represent atmospheric conditions in which some scattering occurs but which are nevertheless dominated by absorption processes. Such conditions are typically associated with light rainfall rates at frequencies less than 50 GHz. Such low values of a are also typical of radiative properties in the vicinity of strong molecular absorption regions such as the 22- and 183-GHz channels near water vapor absorption lines or the 60-GHz channels near the oxygen absorption line.

Values for a increase with both rainfall rate and frequency. More important, however, is the fact that the single scattering albedo for frozen hydrometeors is substantially larger than it is for liquid hydrometeors. At high frequencies, large ice concentrations can produce values as high as $a = 0.98$. The upper limit was chosen at $a = 0.9$, however, because molecular absorbers are always present and prevent a_{tot} in (13) from ever reaching a value close to 1.0.

The asymmetry factor g, which is a measure of the forward peakedness of the scattered radiation, was allowed to take on values of 0.0, 0.25, and 0.5. Radiation scattered from atmospheric constituents becomes strongly peaked in the forward direction when the size of the particles becomes very large in comparison to the wavelength. In the microwave regime, hydrometeors are rarely very large compared to the wavelength (0.1–10 cm), and g consequently rarely exeeds values of 0.5 for the problems considered here. A set of typical values for the asymmetry factor and the single scattering albedo discussed above for a rainfall rate of 16 mm/h was given in Table 1.

Figure 2 shows the brightness temperature differences between the analytical Eddington approximation and the eight-stream discrete ordinate solution. Results are shown for continuous values of the viewing angle θ and optical thickness τ, defined as the extinction coefficient k_{ext} times the height of the cloud. The numerical values shown in Figure 2 represent $\text{Tb}_{\text{edd}} - \text{Tb}_{\text{do}}$. The most obvious conclusion which can be drawn from this figure is that except for very small regions near nadir and very large viewing angles, the Eddington approximation consistently produces brightness temperatures which are slightly too cold. This result is consistent with the findings of *Evans and Stephens* [1990], which compared their "adding and doubling" solution to the Eddington solution and found the Eddington solution to be generally too cold by up to 3°K in one extreme case.

Figure 2 further reveals that for optical thicknesses of less than 0.1 the results from the models tend to agree to within 0.3°K for all studied values of a and g and for all viewing angles. Agreements of better than 1°K are also found consistently if a is small (i.e., $a < 0.1$). The largest differences between the models, however, appear not for the optically thickest clouds nor those having the highest values of the single scattering albedo. Instead they appear at moderate values for each of these quantities. This result is not surprising if one considers the fact that the diffuse radiation within optically thick clouds must become very homogeneous. In this case, the Eddington approximation does not have any problems capturing the angular dependence of the radiation field and is expected to perform well.

The results so far have been for single-layer clouds which were constructed somewhat arbitrarily. They were intended to show the agreements and disagreements between the two radiative transfer solutions under simple circumstances, and to illustrate the difficulties associated in making general remarks concerning the differences in the calculated brightness temperatures. Attention is now shifted to realistic cloud profiles. These were obtained from the cloud mircophysical-dynamical model of *Tao et al.* [1987]. This model supplies a complete atmospheric profile, including temperature, relative humidity, cloud liquid water, cloud ice, precipitable liquid and two classes of precipitable ice (snow and graupel). The resolution of the model is 1.5 km in the horizontal direction and 30 layers in the vertical. In the present calculations, cloud ice, snow, and graupel are combined to a single class of ice. *Marshall-Palmer*, [1948] drop size distributions are used throughout.

The particular simulation considered in this study involved a fast moving squall line over a tropical ocean. The associated rainfall intensities produced at the surface are shown in Figure 3. Comparisons at a viewing angle of 50° for four very distinct rainfall conditions in this simulation, denoted by points *a–d* in Figure 3, are presented explicitly in Table 5. As can be seen, the agreement is quite good for all frequencies.

Comparable results were achieved when all the profiles

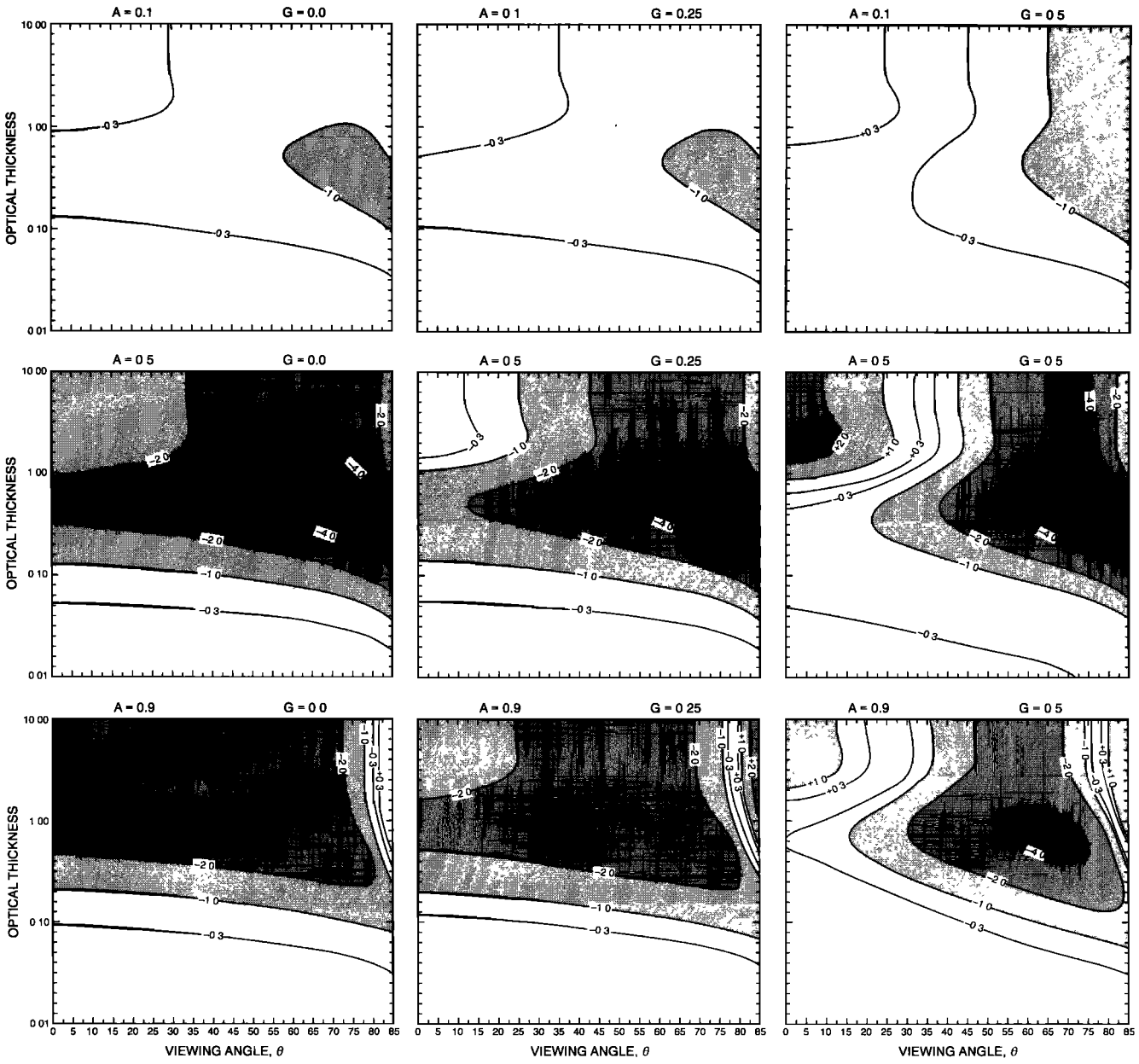

Fig. 2. Brightness temperature difference between Eddington approximation and an eight-stream discrete ordinate solution. Contours are for $TB_{edd} - TB_{do}$ in degrees Kelvin.

along the $x = 17$ grid line were considered. The magnitude of the average deviation or bias, Δ, defined by

$$\Delta = \frac{1}{N_{PTS}} \sum_{i=1}^{N_{PTS}} |TB_{edd} - TB_{do}| \tag{16}$$

is given in Table 6. Considering the range of variability in each of the channels, the average bias shown in Table 6 represents an accuracy of roughly 1%.

4. Discussion

The multiple scattering component of the upwelling radiance is a complicated function of the phase function and the single scattering albedo. Clearly, when a is small, one would expect the Eddington approximation to reproduce brightness temperatures very well. On the other hand, if the phase function does not have a strong forward peak and the scattering cross-section is large, then the diffuse radiance within the cloud quickly becomes nearly isotropic. When this is the case, I_0 in (3) becomes the dominant term in the diffuse radiance expansion, and one would again expect the Eddington solution to give very good results.

Disagreements should therefore exist only in those regions where the optical thickness is large and a and g, are both close to unity. Table 1, which gives typical values for these quantities for moderately heavy rainfalls, shows that the above-mentioned conditions are not well met at microwave frequencies. The asymmetry factor in the microwave regime considered here never exceeds a value of $g = 0.55$. In this

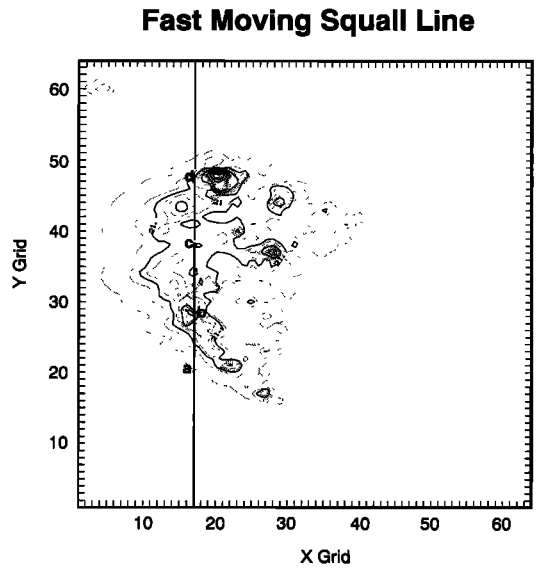

Fig. 3. Surface rainfall contours [mm/h] produced by three-dimensional cloud dynamical models. Points *a–d* are used for detailed radiative transfer comparisons. Rainfall contours are in mm/h.

range of optical thicknesses, and at the viewing angle of 50°, *King and Harshvardhan* [1986] have shown that an Eddington solution performs quite well, even for an asymmetry factor of $g = 0.83$. Good results were also obtained by *Wiscombe and Joseph* [1977] in the visible wavelength when the asymmetry factors was less than 0.5. Thus it is not surprising that the analytical Eddington solution faithfully reproduces the upwelling brightness temperatures.

Large disagreements were found to exist only in a narrow band of viewing angles between 60° and 90°. Here, caution must be excercised because both a and g are large. When the optical thickness is not quite large enough to make the isotropic term of the diffuse radiance the dominant term in the expansion, there appears to be some potential for disagreement. For multilayer clouds, this does not seem to occur very often because the above conditions must be met in a number of consecutive layers for this to occur.

5. CONCLUSIONS

In conclusion, the Eddington solution is found to reproduce brightness temperatures quite well. The errors in the calculated brightness temperatures stemming from the simplified radiative transfer code are far smaller than those introduced by usual uncertainties in the input parameters. Thus for frequencies which are currently being measured, and those which will be measured by upcoming satellite missions, the Eddington approximation should prove more than adequate to handle the bulk of the radiative transfer calculations. However, as pointed out, care should be exercised if absolute accuracies of better than 1% are required. Furthermore, while the computational efficiency of the Eddington method is roughly 20 times greater than the discrete ordinate solution and generally faster than any higher order solution, such increase in efficiency may not always be warranted if only a few calculations are necessary. It should also be noted that the Eddington solution is not well adapted to the transfer of polarized radiation, except in the approximation used by *Wu and Weinman* [1984]. For detailed polarization calculations, the procedures described by *Wilheit et al.* [1977] or *Evans and Stephens* [1990] may be more appropriate.

The simplicity and computational efficiency of the Eddington approximation lends itself primarily to satellite remote sensing applications. Its simplicity, however, also makes it suitable for considering more difficult problems such as the transfer of radiation through three-dimensional structures discussed by *Weinman and Davies* [1978] and *Kummerow and Weinman* [1988]. With the recent availability of realistic three-dimensional cloud structures supplied by cloud dynamical models, these calculations may shed light upon a host questions which cannot be adressed by plane parallel approximations.

The source code and documentation for the analytical Eddington solution discussed in this paper are available from the author on either Apple or IBM diskettes. The code is

TABLE 6. Average Biases Resulting From Eddington Approximation Along $x = 17$ Grid Line Shown in Figure 3

Frequency, GHz	Δ, °K
6.6	0.745
10.7	0.665
18.0	1.569
37.0	1.313
85.6	0.631
183.0	0.557

TABLE 5. Comparisons Between an "Analytical' Eddington Approximation and an Eight-Stream Discrete Ordinate Solution for Selected Profiles Shown in Figure 3

	Frequency, GHz					
Profile	6.6	10.7	18.0	37.0	85.6	183.0
A	154.7	158.8	185.3	201.4	261.1	222.4
	−0.5	−0.8	−1.6	−1.7	−0.9	0.1
B	270.5	258.8	194.1	106.7	91.6	197.3
	0.8	0.2	2.4	−1.2	−0.3	−0.5
C	216.4	266.5	236.3	154.9	127.6	195.3
	−1.5	0.5	0.2	−1.9	−0.9	−0.2
D	204.5	256.7	216.0	100.4	78.5	192.8
	−1.9	0.8	2.6	0.8	−0.3	−0.8

Here, $\theta = 50°$. Top value for each profile is analytical Eddington solution, and botton value is bias which is equal to $TB_{edd} - TB_{do}$.

structured so as not to require any radiative transfer expertise on the part of the user.

Acknowlegments. The author would like to express his gratitude to Warren Wiscombe for supplying the discrete ordinate model code used in this study, Wei-Kuo Tao for supplying cloud dynamical model output, and Jim Wienman for many helpful discussions. Lafayette Long was most helpful in the preparation of the figures.

REFERENCES

Adler, R. F., and A. J. Negri, A satellite infrared technique to estimate tropical convective and stratiform rainfall, *J. Appl. Meteorol.*, *27*, 30–51, 1988.

Arkin, P. A., and B. Meisner, The relationship between large-scale convective rainfall and cold cloud over the western hemisphere during 1982–1984, *Mon. Weather Rev.*, *115*, 51–74, 1987.

Coakley, J. A., Jr., and P. Chylek, The two-stream approximation in radiative transfer: Including the angle of the incident radiation, *J. Atmos. Sci.*, *32*, 409–418, 1974.

Evans, K. F., and G. L. Stephens, Polarized radiative transfer modeling: An application to microwave remote sensing of precipitation, *Atmos. Sci. Pap. 461*, Dep. of Atmos. Sci., Colo. State Univ., Fort Collins, 1990.

Hollinger, J., R. Lo, G. Poe, R. Savage, and J. Pierce, *Special Sensor Microwave/Imager User's Guide*, 120 pp., Naval Research Laboratory, Washington, D. C., 1987.

Inoue, T., An instantaneous delineation of convective rainfall areas using split window data of the NOAA-7 AVHRR, *J. Meteorol. Soc. Jpn.*, *65*, 469–481, 1987.

King, M. D., and Harshvardhan, Comparative accuracy of selected multiple scattering approximations, *J. Atmos. Sci.*, *43*, 784–801, 1986.

Kummerow, C., and J. A. Weinman, Determining microwave brightness temperatures from horizontally finite, vertically structured clouds, *J. Geophys. Res.*, *93*, 3720–3728, 1988.

Marshall, J. S., and W. M. Palmer, The distribution of raindrops with size, *J. Meteorol.*, *5*, 165–166, 1948.

Mugnai, A., and E. A. Smith, Radiative transfer to space through a precipitating cloud at multiple microwave frequencies, I, Model description, *J. Appl. Meteorol.*, *27*, 1055–1073, 1988.

Shettle, E. P., and J. A. Weinman, The transfer of solar irradiance through inhomogeneous turbid atmospheres evaluated by Eddington's approximation, *J. Atmos. Sci.*, *27*, 1048–1055, 1970.

Simpson, J., R. F. Adler, and G. North, A proposed tropical rainfall measuring mission (TRMM) satellite, *Bull. Am. Meteorol. Soc.*, *69*, 278–295, 1988.

Spencer, R. W., A satellite passive 37 GHz scattering based method for measuring oceanic precipitation, *J. Clim. Appl. Meteorol.*, *25*, 754–766, 1986.

Staelin, D. A., Measurements and interpretation of the microwave spectrum of the terrestrial atmosphere near 1 centimeter wavelength, *J. Geophys. Res.*, *71*, 2875–2881, 1966.

Stamnes, K., S.-C. Tsay, W. Wiscombe, and K. Jayaweera, Numerically stable algorithm for discrete-ordinate-method radiative transfer in multiple scattering and emitting layered media, *Appl. Opt.*, *27*, 2502–2509, 1988.

Stephens, G. L., Radiative transfer through arbitrary shaped optical media, I, A general method of solution, *J. Atmos. Sci.*, *45*, 1818–1836, 1988.

Tao, W.-K., J. Simpson, and S.-T. Soong, Statistical properties of a cloud ensemble: A numerical study, *J. Atmos. Sci.*, *44*, 3175–3187, 1986.

Ulaby, F. T., R. K. Moore, and A. K. Fung, *Microwave remote sensing: Active and Passive*, vol. I, *Microwave Remote Sensing Fundamentals and Radiometery*, 456 pp., Addison-Wesley, Reading, Mass., 1981.

Weinman, J. A., and R. Davies, Thermal microwave radiances from horizontally finite clouds of hydrometeors, *J. Geophys. Res.*, *83*, 3099–3107, 1978.

Wilheit, T. T., A. T. Chang, M. S. V. Rao, E. B. Rodgers, and J. S. Theon, A satellite technique for quantitatively mapping rainfall rates over the ocean, *J. Appl. Meteorol.*, *16*, 551–560, 1977.

Wiscombe, W. J., and J. H. Joseph, The range of validity of the Eddington approximation, *Icarus*, *32*, 362–377, 1977.

Wu, R., and J. A. Weinman, Microwave radiances from precipitating clouds containing aspherical ice, combined phase, and liquid hydrometeors, *J. Geophys. Res.*, *89*, 7170–7178, 1984.

C. Kummerow, Laboratory for Atmospheres, Goddard Space Flight Center, Greenbelt, MD 20771.

(Received October 25, 1991;
revised September 29, 1992;
accepted October 12, 1992.)